In House Development of Contact Microphone Based Wearable Device for Knee Joint Health Assessment Using Vibroarthrography
Vibroartrografi Kullanılarak Diz Eklemi Sağlığı Değerlendirmesi için Kontak Mikrofon Tabanlı Giyilebilir Cihazın Kurum İçi Geliştirilmesi

Dhirendra Kumar Verma[1,*], Mirsaidin Hussain[1], Poonam Kumari[1], Subramani Kanagaraj[1]
[1]Department of Mechanical Engineering, Indian Institute of Technology Guwahati, North Guwahati, Guwahati, Assam 781039, India
ORCID: 0000-0002-3954-3198, 0000-0002-9631-7277, 0000-0002-0984-5347, 0000-0002-2050-1887
E-mails: vermadk.iimt@gmail.com, mirsaidin@gmail.com, kpmech@iitg.ac.in, kanagaraj@iitg.ac.in
*Corresponding author.

***Abstract*—Nowadays, bone joint disorders are very common in humans. The knee joint abnormality often comes with the increasing age of people. Cartilage degradation and rubbing action of the femoral condyle to the tibial condyle generates the knee joint sounds and this stage turns into osteoarthritis. There are pre-existing diagnosis methods available like X-ray, MRI, etc. but they have their limitations. Some treatment methods are invasive and some are semi-invasive. Early diagnosis of osteoarthritis is possible using vibroarthrography which is a purely non-invasive method and sensor signal output can be featured as an informative tool for next-level treatment. In this study, a contact microphone-based wearable device has been fabricated for knee joint health monitoring and joint angle-based sensor voltage output is characterized. The result of fast Fourier transformation from healthy subjects is observed to be from 0 Hz-100 Hz and short-term Fourier transformation is performed for the obtained decibel value from 40-45 dB. The result of a pathological knee is studied in spectral density analysis and observed a continuous emission of joint sound and signal power distribution is observed over the frequency range of 0 Hz - 500 Hz.**

***Keywords*—knee joint anatomy; contact microphone; osteoarthritis; vibroarthrography**

***Özetçe*—Günümüzde kemik eklem rahatsızlıkları insanlarda çok yaygındır. Diz eklemi anormalliği genellikle artan yaşla birlikte gelir. Kıkırdak degradasyonu ve femoral kondilin tibial kondile sürtünme hareketi diz eklemi seslerini oluşturur ve bu evre osteoartrite dönüşür. Röntgen, MRI vb. gibi önceden var olan tanı yöntemleri mevcuttur ancak bunların sınırlamaları vardır. Bazı tedavi yöntemleri invaziv, bazıları ise yarı invazivdir. Osteoartritin erken teşhisi, tamamen non-invaziv bir yöntem olan vibroartrografi kullanılarak mümkündür ve sensör sinyal çıkışı, bir sonraki seviye tedavi için bilgilendirici bir araç olarak öne çıkarılabilir. Bu çalışmada, diz eklemi sağlığının izlenmesi için kontak mikrofon tabanlı giyilebilir bir cihaz üretilmiş ve eklem açısına dayalı sensör voltaj çıkışı karakterize edilmiştir. Sağlıklı deneklerden hızlı Fourier dönüşümünün sonucunun 0 Hz-100 Hz arasında olduğu gözlenir ve 40-45 dB arasında elde edilen desibel değeri için kısa süreli Fourier dönüşümü yapılır. Patolojik bir diz sonucu, spektral yoğunluk analizinde incelenir ve 0 Hz- 500 Hz frekans aralığında sürekli bir eklem sesi emisyonu ve sinyal güç dağılımı gözlemlenir.**

***Anahtar Kelimeler*—diz eklemi anatomisi; iletişim mikrofonu; kireçlenme; vibroartrografi**

I. Introduction

The knee joint is the largest load bearer in the human body. It has a complex interplay between four major bones, femur, tibia, patella, and fibula. These bones are insulated from each other by the meniscus and articular cartilages. The joint is filled with synovial fluid and the ligaments provide strength and stability to the bones (Fig. 1). The articular cartilage produces cushioning effect to the knee bones during dynamic movements of the joint and majorly reduces the overall friction. The complete articulation can be simplified into three unique and individual joints or motions like tibio-femoral, patello-femoral, and tibio-fibular. These individual segments do relative motion between each other by making one as a reference in the sliding and gliding action of the joint [1].

In our daily life activities, the maximum engaged and most participated body part is the knee joint. There is always a high probability of the joint disorder and it may happen due to several reasons. Predominantly there are trauma-related injuries in which heavy-duty physical activity may be a cause of joint dysfunction. Joint dislocations due to fractures, ligamental

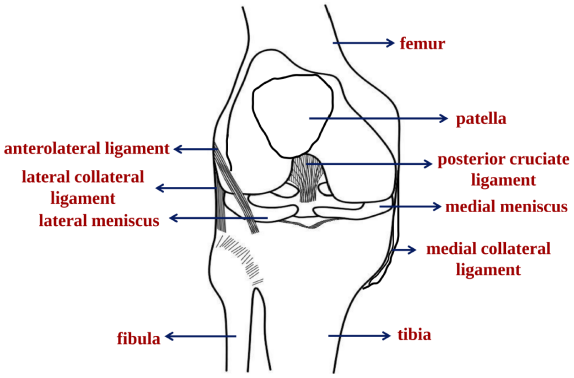

Figure 1: Knee Joint Anatomy

injuries, meniscal tears, and tendon tears are the primary cause of joint injury [2]. The second is the autoimmune disorder like rheumatoid arthritis. It is a chronic disorder and systematic inflammation of the synovial membrane which results in progressive and permanent bone erosion and results in a painful condition in humans. The common symptoms are an increase in temperature, joint tenderness, swelling, and pain [3]. The third and the major is osteoarthritis which often occurs in both males and females but is very common in females. It is an age-associated and irreversible disorder that may lead to total knee replacement conditions if early diagnosis is not performed. In this disorder, the structural tissues change and with the slow progression, it turns into a chronic disease. Osteoarthritis (OA) mainly occurs due to cartilage degradation and if adequate treatment is not taken on time then it turns into an irreversible phase [4]–[6].

There are several diagnosis methods for OA detection that are already available but each has its own limitations. X-ray radiograph is the conventional technique but it does not predict the articular cartilage degeneration and does not identify the cartilage lesion on it. It mainly shows the joint space narrowing [7]. Another detection method is Ultrasound Imaging in which high-frequency transducers are used to visualize the cartilage damage. It is susceptible to detect changes in soft tissue and joint space narrowing [8]. This non-invasive method is limited by its acoustic window to visualize the cartilage and is also not able to penetrate the bony cortex [9]. Optical Coherence Tomography (OCT) is used to detect in-vivo cartilage damage in micrometre resolutions. It is infrared-based imaging and can produce a three-dimensional image to interpret the joint tissue microstructure. Sometimes this becomes more invasive when used in the combination of arthroscopy and T2 MRI and a very skilled operator is required [10]. Another very popular and non-invasive examination method is the Magnetic Resonance Imaging (MRI) which is useful to detect the defects on the articular cartilage surfaces. Though this diagnosis method is very popular but has certain limitations like it is less sensitive to detect damages to ligaments as well as an extent level of cartilage degeneration can not be observed. It is also a costly procedure [11]. The above-discussed methods have their proven efficacy with certain limitations like they are not suitable in daily life health assessment in real-time dynamic joint movements and are limited to taken home healthcare system in the current scenario [12]. The early diagnosis of knee joint helps the physicians for moving forward with suitable therapeutic procedures and then they refer the patient to the interventions, medicines, or surgical procedures. In most cases, the proper early care can delay the joint degeneration, and to accomplish this need, vibroarthrography is the most effective and recognized diagnosis method [13], [14]. It is a fast-growing technology in knee joint auscultation and detects the sound from a pathological knee. The simple mechanism of sound generation is due to the lack of synovial fluid inside the joint and cartilage deterioration primarily due to age and obesity [15]. It is the most common and dominating disease in females. Acoustic signals are generated due to the rubbing contact of the femoral condyle with the tibial condyle and gliding of the patella. Mostly, the medial side of the joint is often affected because the line of action of load passes through the medial side of the joint in a normal gait cycle [16], [17]. The details in the field of vibroarthrography and its development as a diagnostic tool can be found in the referred literature in this study [18]–[22].

II. Materials & Methods

A. Device Development

In this work, the initial circuit is fabricated on the bread-board by using primary components like jumper wires, resistors, a push-button DPDT (double-pole, double-throw) switch, a light-emitting diode (LED), power supply, Arduino Nano, SD card module, and a contact microphone (CM01-B). The selected microphone used for this study is consist of a piezo-electric sensor that can sense the acoustic emission in the range of limiting frequency from 8 Hz to 2.2 kHz. Arduino Nano is a microcontroller board, and as the name indicates, it is small, compact, and highly compatible with breadboard and other electronic components. It is available with two different versions of the microcontroller, i.e., Atmel ATmega168 and ATmega 328. There are 14 digital pins on the Nano board. All 14 digital pins can be used for input and output modes at 5V operating voltage. Each pin can deliver or receive a maximum of 40 mA current. Apart from this, the other pins have their specific use, like RX0 and TX1 are used to receive and transmit serial data, respectively, and are also said to be serial communication pins [23]. The primary circuit is successfully fabricated and the signal is amplified for knee joint sound detection. A schematic of the primary circuit is shown in (Fig. 2). The fabricated circuit is then converted into a printed circuit board (PCB) and a final version of the wearable device has been fabricated using 3D printing of the casing and assembly of components (Fig. 3).

B. Participants

In this study, twenty-four healthy subjects (sixteen males (30.31 ± 12.15 years, 66.73 ± 10.10 kg, 170.19 ± 8.26 cm) and eight females (28.00 ± 4.96 years, 62.21 ± 9.78 kg, 154.68 ± 5.95 cm)) are recruited for their participation and

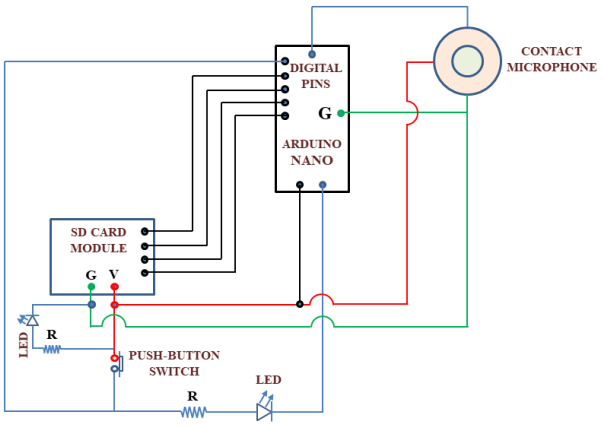

Figure 2: Circuit Schematic

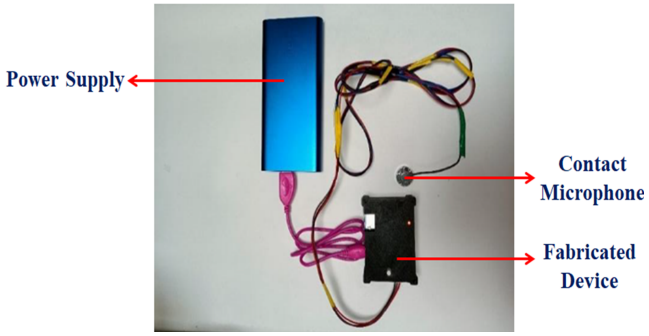

Figure 3: Fabricated Device

confirmed with no lower extremity injury. Simultaneously, two pathological male subjects (50.00 ± 18.34 years, 72.85 ± 3.47 kg, 163.75 ± 10.25 cm) are also recruited for identification of the OA suspicion and confirmed with a prior medical history of knee joint pain. Each participation is confirmed with standard inclusion and exclusion criteria followed by their written ethical consent. The study is approved by the Institute Human Ethical Committee (IHEC), IIT Guwahati.

C. Sensor Positioning

It is always critical to fix the sensor on the skin surface in a correct manner and to record acoustic signals accurately. Previous studies reported the optimized placement location at the medial condyle of the patella, i.e. slightly below the midline of the patella. This point is identified as the closest one nearby to the contact area during joint articulation. It is a stable position during joint movement and does not affect by actual joint motion [24], [25]. Along with the contact microphone, a self-fabricated inertial measurement unit (IMU) based digital goniometer is also placed on the mid of the thigh and the shank bone on each subject in the sagittal plane.

D. Data Collection

During the data collection individual subject is trained to perform an active knee joint weight-bearing sit-stand-sit (S-T-S) exercise for recording the vibroarthrographic signals. The subjects are asked to do three S-T-S cycles in one trial for the data collection and synchronized with the metronome. Each cycle consists of the following four phases of motion as shown in figure 4:

- Ascending-Acceleration (AA)
- Ascending-Deacceleration (AD)
- Descending-Acceleration (DA)
- Descending-Deacceleration (DD)

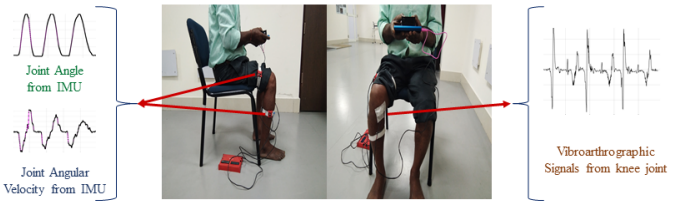

Figure 4: Sensor Positioning and Test Procedure

This device gives the output in terms of voltage which is produced due to the knee joint auscultation during the S-T-S exercise and the real-time data is stored in the attached SD card with the device. The knee kinematics parameters are obtained from the digital goniometer. The primary function of the digital goniometer in this knee joint health assessment using vibroarthrography is to identify the variation of voltage generated with respect to four motion phases.

III. Results and Discussion

A. Sensor Output and Motion Phase Identification

Fig. 5 shows the output of the contact microphone-based wearable device and the digital goniometer from an active knee joint S-T-S exercise of a healthy subject in terms of voltage, knee joint angle, and angular velocity and are plotted in the same time series to distinguish the voltage in different phases. Here the output voltage obtained is found to be in the range of 0 mV to 6 mV, for the joint angular movement between 0° to 90° and the simultaneous joint angular velocity in the range of 0°/sec to 80°/sec. This same time series distinguishes the voltage in different phases w.r.t. joint movement during the exercise performed. From Fig. 5,it can be seen that during the exercise, there are differences among the vibroarthrographic signals in four phases, the output voltage becomes higher while the subject proceeds towards the standing position from the sitting position.

B. Fourier Transform Analysis

The obtained data from the microphone in terms of voltage vs time series is post-processed by using MATLAB. Signal processing features are obtained and the frequency spectrum is analyzed. During data processing the ‘N’ point, time-domain

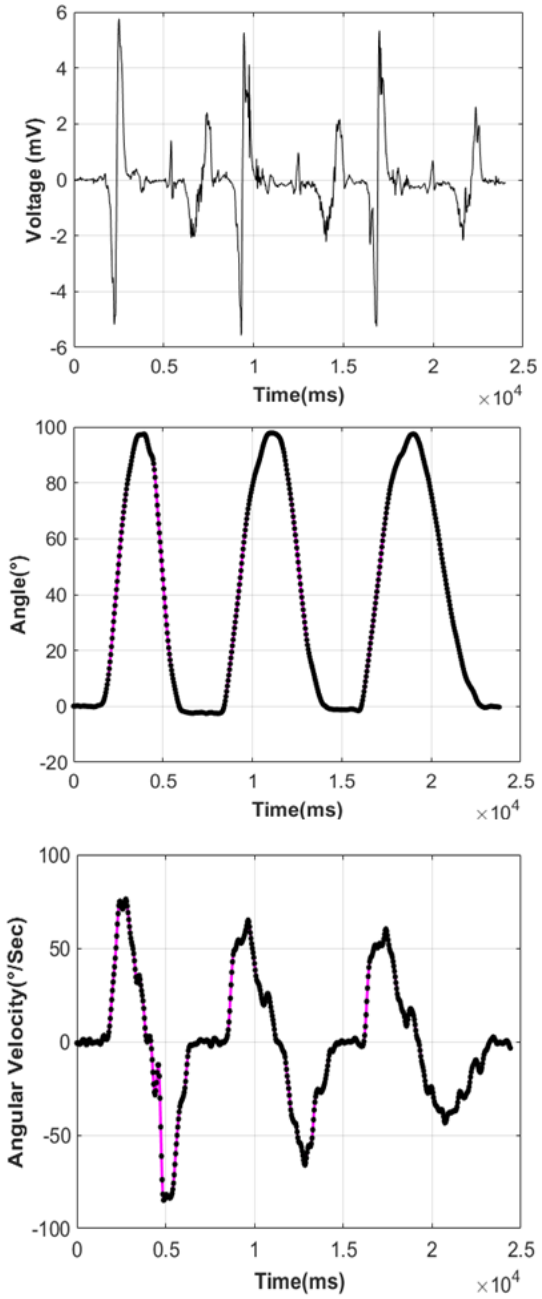

Figure 5: Joint Angle Based Vibroarthrography

signals are decomposed into 'N' time-domain single point signals, and then corresponding 'N' frequency spectrums are calculated. This results in the contained frequency of the input signal on the fast Fourier transform (FFT) plot. Further, the Short-term Fourier transform (STFT) is obtained for all segments of the frequency spectra on a single plot. This STFT is a very powerful way to represent all contained frequencies in the scale of time, frequency, and signal amplitude together. Also, it initially divides the spectrum into small segments and then combinedly shows the frequency distributions throughout the recorded signal with its amplitude distribution. Fig. 6 and 7 show the FFT of the vibroarthrographic signals, collected when a healthy and an unhealthy subject performed the weight-bearing S-T-S exercise while STFT is shown in Fig. 8 and 9 respectively. As shown in Fig. 6 and 7, there are peak-frequency components when a subject performs a movement in a standing position from the sitting position which is also justified by the higher voltage value as shown in Fig. 5 during the same phase. Fig. 6 and 7 show the difference in frequency peaks between the healthy and unhealthy subjects, respectively. It is observed that in both the cases the obtained peak frequencies are different and less than 100 Hz but there is a significant difference in the signal amplitude. These results are in line with the published literature [26]. In Fig. 8 and 9, the spectrogram of STFT of the output voltage of a healthy and an unhealthy subject is shown respectively to provide the time-localized frequency information in which frequency components of a signal vary over time. It is also been observed that the peak amplitude obtained for a healthy subject is 43 dB and for a pathological subject is 63 dB approximately which is shown in the following graphs.

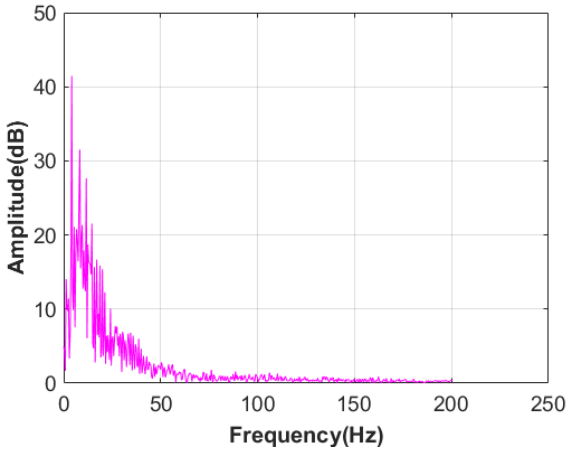

Figure 6: Frequency Analysis from Healthy Knee

Fig. 10 shows the violin plots for the sixteen healthy (male), eight healthy (female), and two pathologies (male) subjects. Here, the maximum amplitude (in dB level) data is considered with a kernel density distribution with a box plot. kernel density distribution, a statistical technique is used to map the real-valued function to the weighted average of the observed neighboring data. The plots show the median (a green dot on

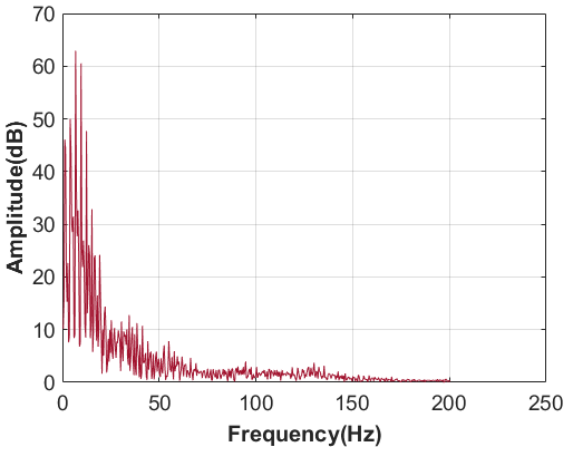

Figure 7: Frequency Analysis from Pathological Knee

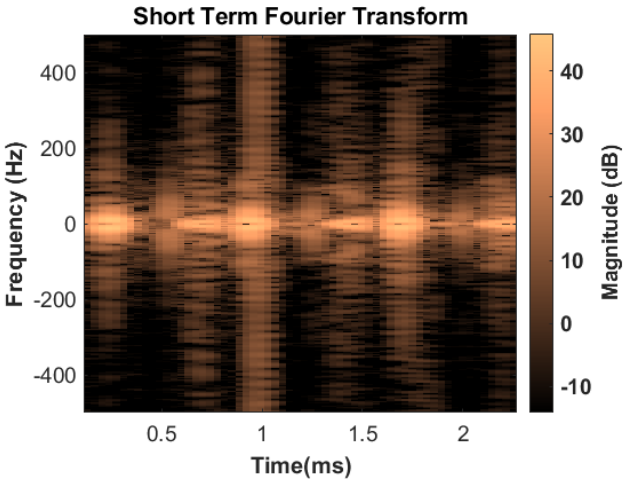

Figure 8: Frequency Spectogram from Healthy Knee

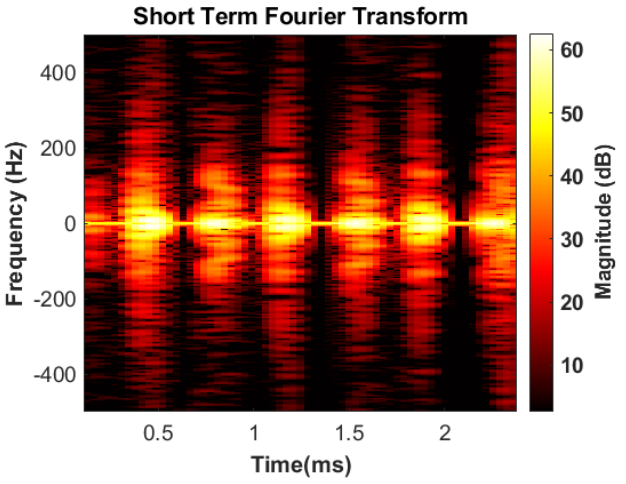

Figure 9: Frequency Spectogram from Pathological Knee

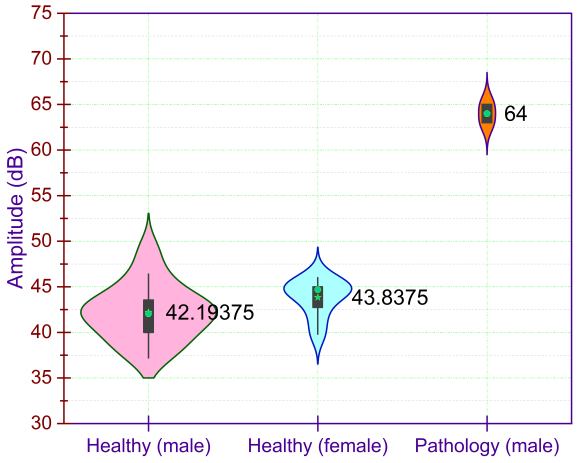

Figure 10: Violin Plots for Different Subject Groups

the violin plot) with the interquartile range (a black bar at the center of the plot). In these plots, the corresponding mean (a green star on the violin plot) of the amplitudes is also shown with its magnitude for each group. From the violin plots, the maximum amplitude of acoustic emission obtained from the fabricated device is obtained to be in the range of 40-45 dB and 60-65 dB for the healthy subjects and pathology subjects, respectively.

C. Spectral Density Analysis

Power spectral density is used to quantify the spectral power over the interested frequency band. It also gives the signal power variations over the time scale of the order of 1/Hz. Fig. 11 and 12 represents the waterfall plot or a time-frequency observation in the form of the spectrogram. Here the signal duration in seconds and contained frequencies in Hz are represented in the XY plane while Z-axis represents power spectral density (PSD) obtained from a pathological knee during the experiments in the (dB/Hz) scale for each time-frequency frame. In Fig. 11, it is observed that the spectral signal power distribution for a healthy knee the gain in frequency is obtained at three certain locations in the time duration and it is because of the particular joint articulation. However, the pathological knee exhibits continuous frequencies as shown in Fig. 12 over the different frequencies from 0 Hz to 500 Hz. It represents the continuous generation of the vibration signals during the joint articulation throughout the signal acquisition period (0 s-2.5 s) and indicates the unhealthy knee joint condition.

IV. Conclusion

In this work, a contact microphone-based wearable device has been successfully fabricated using an Arduino nano microcontroller and other necessary electronic components. The primary circuit is tested and calibrated and further converted into a printed circuit board (PCB). The device is successfully tested on healthy and pathological subjects by analyzing their knee joint sounds by employing vibroarthrography. Raw joint

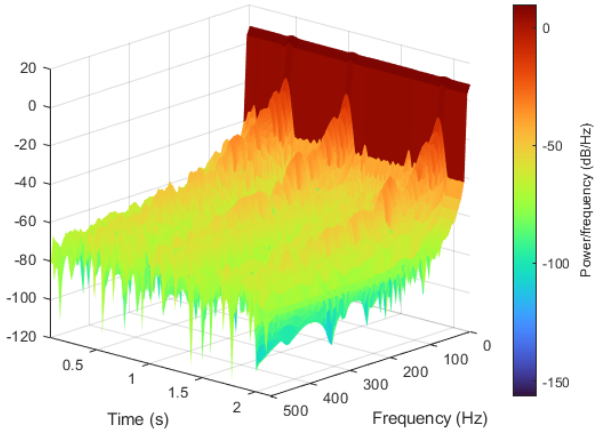

Figure 11: Spectral Density from Healthy Knee

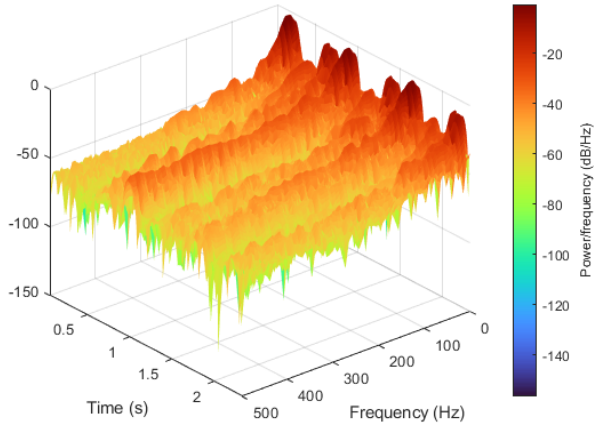

Figure 12: Spectral Density from Pathological Knee

signals are stored in the device. After analog to digital conversion and postprocessing of the data in MATLAB R2021a version software, essential signal features are obtained. Sensor output up to 6 mV along with the joint articulation in the range of 0°-90° is obtained in all subjects during experiments. The signal time-frequency analysis reveals a significant difference between a healthy and pathological knee and indicates that the pathological knee emits a continuous vibration signal during data sampling. It can be concluded that healthy subjects emit the lower decibel level of amplitude (40-45 dB) compared to that of pathological subjects (60-65 dB).

Author Contributions

This paper is a part of *First Author*'s PhD research work. *Second Author* is the project staff, *Third and Fourth Authors* are the supervisor and co-supervisor of the PhD research work. *First and Second Authors* equally contributed on writing the paper. Funding resources, supervision, review, manuscript correction, and editing are done by *Third and Fourth Authors*.

Acknowledgements

The authors gratefully acknowledge the North East Centre for Biological Sciences and Healthcare Engineering (NECBH) and the clinical staff of the Gait Lab at IIT Guwahati for facilitating a platform for conducting the experiments. The authors are also indebted to the industrial research partner "Olatus system private limited" at IIT Guwahati for contributing to the circuit development and PCB fabrication of the wearable device.

Funding

This work is supported by DST grant number TDP/BDTD/03/2021(G) for "Development and testing of a wearable device for the early detection of a cartilage damage in a knee stepping towards an osteoarthritis condition using acoustic emission" and New Generation Innovation and Entrepreneurship Development Centre (NewGen IEDC), Department of Science and Technology (DST), Government of India.

Conflict of Interest

The authors declared no potential conflicts of interest concerning the research, authorship, and publication of this article.

References

[1] Bull AMJ, Amis AA. Knee joint motion: Description and measurement. Proceedings of the Institution of Mechanical Engineers, Part H: Journal of Engineering in Medicine 1998; 212(5): 357-372.

[2] Yanagawa T, Shelburne K, Serpas F, Pandy M. Effect of hamstrings muscle action on stability of the ACL-deficient knee in isokinetic extension exercise. Clinical Biomechanics 2002; 17(9-10): 705-712.

[3] Conigliaro P, Triggianese P, De Martino E, Fonti GL, Chimenti MS, Sunzini F, Viola A, Canofari C, Perricone R. Challenges in the treatment of rheumatoid arthritis. Autoimmunity Reviews 2019; 18(7): 706-713.

[4] Ahn JH, Kang DM, Choi KJ. Risk factors for radiographic progression of osteoarthritis after partial meniscectomy of discoid lateral meniscus tear. Orthopaedics & Traumatology: Surgery & Research 2017; 103(8): 1183-1188.

[5] Jones MH, Spindler KP. Risk factors for radiographic joint space narrowing and patient reported outcomes of post-traumatic osteoarthritis after ACL reconstruction: data from the MOON cohort. Journal of Orthopaedic Research 2017; 35(7): 1366-1374.

[6] Cibere J, Sayre EC, Guermazi A, Nicolaou S, Kopec JA, Esdaile JM, Thorne A, Singer J, Wong H. Natural history of cartilage damage and osteoarthritis progression on magnetic resonance imaging in a population-based cohort with knee pain. Osteoarthritis and Cartilage 2011; 19(6): 683-688.

[7] Nagaosa Y, Lanyon P, Doherty M. Characterisation of size and direction of osteophyte in knee osteoarthritis: A radiographic study. Annals of the Rheumatic Diseases 2002; 61(4): 319-324.

[8] Doria AS. State-of-the-art imaging techniques for the evaluation of haemophilic arthropathy: Present and future. Haemophilia 2010; 16(s5): 107-114.

[9] Ostergaard M, Court-Payen M, Gideon P, Wieslander S, Cortsen M, Lorenzen I, Henriksen O. Ultrasonography in arthritis of the knee: A comparison with MR imaging. Acta Radiologica 1995; 36(1): 19-26.

[10] Ibne Mokbul M. Optical coherence tomography: Basic concepts and applications in neuroscience research. Journal of Medical Engineering 2017; 2017: 3409327.

[11] Krakowski P, Nogalski A, Jurkiewicz A, Karpiński R, Maciejewski R, Jonak J. Comparison of diagnostic accuracy of physical examination and MRI in the most common knee injuries. Applied Sciences 2019; 9(19): 4102.

[12] Ciklacandir S, Isler Y. A cost-effective solution for real-time measurement of human joint angles. Karaelmas Science and Engineering Journal, ACCEPTED, 2021.

[13] Wu Y, Krishnan S, Rangayyan RM. Computer-aided diagnosis of knee-joint disorders via vibroarthrographic signal analysis: A review. Critical Reviews in Biomedical Engineering 2010; 38(2): 201-224.

[14] Wu Y, Cai S, Yang S, Zheng F, Xiang N. Classification of knee joint vibration signals using bivariate feature distribution estimation and maximal posterior probability decision criterion. Entropy 2013; 15(4): 1375–1387.

[15] Falkowski K, Skiba G, Czerner M, Szmajda M and Bączkowicz D. Effects of viscosupplementation on knee joint arthrokinematics - Pilot study. Ortop Traumatol Rehabil 2018; 20(5): 409–419.

[16] van den Borne MPJ, Raijmakers NJH, Vanlauwe J, Victor J, de Jong SN, Bellemans J, Saris DBF. International Cartilage Repair Society (ICRS) and Oswestry macroscopic cartilage evaluation scores validated for use in Autologous Chondrocyte Implantation (ACI) and microfracture. Osteoarthritis and Cartilage 2007; 15: 1397–1402.

[17] Karpiński R, Machrowska A, Maciejewski M. Application of acoustic signal processing methods in detecting differences between open and closed kinematic chain movement for the knee joint. Applied Computer Science 2019; 15: 36–48.

[18] Reddy NP, Rothschild BM, Mandal M, Gupta V, Suryanarayanan S. Noninvasive acceleration measurements to characterize knee arthritis and chondromalacia. Annals of Biomedical Engineering 1995; 23(1): 78-84.

[19] Shen Y, Rangayyan RM, Bell GD, Frank CB, Zhang YT, Ladly KO. Localization of knee joint cartilage pathology by multichannel vibroarthrography. Medical Engineering & Physics 1995; 17(8): 583-594.

[20] Maussavi ZM, Rangayyan RM, Bell GD, Frank CB, Ladly KO. Screening of vibroarthrographic signals via adaptive segmentation and linear prediction modeling. IEEE Transactions on Biomedical Engineering 1996; 43(1): 15.

[21] Rangayyan RM, Krishnan S, Bell GD, Frank CB, Ladly KO. Parametric representation and screening of knee joint vibroarthrographic signals. IEEE Transactions on Biomedical Engineering 1997; 44(11): 1068-1074.

[22] Tanaka N, Hoshiyama M. Vibroarthrography in patients with knee arthropathy. Journal of Back and Musculoskeletal Rehabilitation 2012; 25(2): 117-122.

[23] Agus K. Arduino Nano A Hands-on Guide for Beginner. PE Press, 2019.

[24] Song CG, Kim KS, Seo JH. Non-invasive monitoring of knee pathology based on automatic knee sound classification. In Proceedings of the World Congress on Engineering and Computer Science, October 20-22, 2009, San Francisco, USA.

[25] Befrui N, Elsner J, Flesser A, Huvanandana J, Jarrousse O, Le T N, Müller M, Schulze W H, Taing S, Weidert S. Vibroarthrography for early detection of knee osteoarthritis using normalized frequency features. Medical & Biological Engineering & Computing 2018; 56(8): 1499-1514.

[26] Ye Y, Wan Z, Liu B, Xu H, Wang Q, Ding T. Monitoring deterioration of knee osteoarthritis using vibration arthrography in daily activities. Computer Methods and Programs in Biomedicine 2022; 213: 106519.